Sensors and Actuators B 154 (2011) 59–66

Contents lists available at ScienceDirect

Sensors and Actuators B: Chemical

journal homepage: www.elsevier.com/locate/snb

Microfluidic aptameric affinity sensing of vasopressin for clinical diagnostic and therapeutic applications

ThaiHuu Nguyen [a], Renjun Pei [b], Donald W. Landry [b], Milan N. Stojanovic [b], Qiao Lin [a,*]

[a] Department of Mechanical Engineering, Columbia University, New York, NY 10027, United States
[b] Division of Clinical Pharmacology and Experimental Therapeutics, Department of Medicine, Columbia University, New York, NY 10032, United States

ARTICLE INFO

Article history:
Available online 20 October 2009

Keywords:
Arginine vasopressin
Aptamer
Aptasensor
Biosensor
Enrichment
Isocratic elution
Mass spectrometry

ABSTRACT

We present a microfluidic aptameric biosensor, or aptasensor, for selective detection of clinically relevant analytes with integrated analyte enrichment, isocratic elution and label-free detection by mass spectrometry. Using a microfluidic platform that is coupled to matrix assisted laser desorption/ionization mass spectrometry (MALDI–MS), we demonstrate specific purification, enrichment, and label-free detection of trace amounts of arginine vasopressin (AVP), a peptide hormone that is responsible for arterial vasoconstriction. During extreme physical trauma, in particular immunological shock or congestive heart failure, AVP is excreted abnormally and is hence a biomarker for such conditions. The device uses an aptamer, i.e., an oligonucleotide that binds specifically to an analyte via affinity interactions, to achieve highly selective analyte capture and enrichment. In addition, via thermally induced reversible disruption of the aptamer-analyte binding, the device can be easily regenerated for reuse and allows isocratic analyte elution, i.e., release and collection of analytes using a single aqueous solution. Furthermore, the device is coupled to MALDI–MS using a microfluidic flow gate, which directs the eluted analyte onto a MALDI sample plate for mass spectrometry. We first perform systematic characterization of kinetic and thermal release properties, as well as the overall timescale of the assay, using fluorescently labeled AVP. We then demonstrate MALDI–MS detection of unlabeled AVP at clinically relevant concentrations approaching 1 pM.

1. Introduction

Biosensors are widely used for the detection and analysis of biomolecules that are disease relevant biomarkers such as genes, proteins, and peptides. Typically, they consist of a molecular recognition component and a transducer converting the binding event into a measurable physical signal [1]. A particularly important class of biosensors comprises affinity biosensors, which rely on highly selective affinity receptors, such as aptamers [2], to recognize target biomolecules. Aptamers are oligonucleotides that recognize target molecules specifically by highly selective affinity interaction; they are isolated through a synthetic procedure called systematic evolution of ligands by exponential enrichment (SELEX), whereby very large populations of random sequence oligomers (DNA or RNA libraries) are screened against the target molecule in an iterative procedure [3]. Aptamers have been developed to target a variety of biomolecules (e.g., small molecules [4], peptides [5], and proteins [6]) in diverse applications, such as target validation [7], drug discovery [8], and in particular, diagnostics [9] and therapy [10]. The intense attention received by aptamers can be attributed not only to their high specificity, but also to characteristics that are lacking in more established affinity receptors such as enzymes, lectins, and antibodies [11]. These include synthetic availability, enhanced stability at room temperature, and more easily modified terminal ends for attachment to stationary surfaces. Moreover, aptamer-target binding is generally reversible under changes in environmental parameters such as pH and temperature [12], which can be exploited to allow controlled release and recovery of target biomolecules as well as sensor regeneration.

Microfluidics technology has been used to enable antibody- and enzyme-based biosensors that are miniaturized and can potentially offer drastically improved performance [13,14]. However, application of microfluidics to aptasensing has been relatively scarce. In an early example, microbeads were conjugated with an aptamer via a photo-cleavable linker, and packed in a microfluidic chip to extract HCV replicase, which was then eluted together with the aptamer by UV irradiation for analysis by mass spectrometry [15,16]. An aptasensor was constructed for the specific detection of Thermus aquaticus DNA polymerase by monitoring the deflection of a microcantilever induced by surface stress changes due

* Corresponding author at: Department of Mechanical Engineering, Columbia University, 500 W 112th St, Mudd Rm 220, New York, NY, 10027, United States. Tel.: +1 212 854 1906.
E-mail address: qlin@columbia.edu (Q. Lin).

0925-4005/$ – see front matter © 2009 Elsevier B.V. All rights reserved.
doi:10.1016/j.snb.2009.10.032

to affinity binding [19]. Microfluidic aptasensors were developed for aptamer-based cocaine detection using electrochemical detection [17] or fluorescence resonance energy transfer methods [18]. A Love-wave microfluidic aptasensor was microfabricated to detect multifunctional serine protease thrombin and Rev peptide [20]. In related work, nanostructures such as single-walled carbon nanotubes [21] or gold nanowires [22] have been functionalized with aptamers to detect the protein thrombin. These works, while primarily focused on model analytes, and have shown the promise of microfluidic-based aptasensors for clinical applications.

Among the broad clinical applications of aptasensors, a particularly interesting example involves detection of arginine vasopressin (AVP) for the diagnosis and therapy of septic shock (induced by severe infection) and congestive heart failure [23], conditions that restrict adequate perfusion by the cardiovascular system in order to maintain organ functionality. Both disorders are indicated by elevated levels of AVP, a cyclic polypeptide neurohormone that is synthesized in the hypothalamus and promotes vasoconstriction [24]. Specifically, physiological concentrations of AVP in plasma markedly increases up to 10-fold that of average levels (5–10 pM) in order to maintain arterial pressure and hence, blood perfusion. As shock progresses, however, the initial abundance of AVP in plasma decreases [25]. Thus, the ability to monitor and control AVP over time would reveal the homeostatic stasis of the patient, and could potentially provide therapeutic solutions. Current clinical platforms for vasopressin include immunoradiometric assays (IRA) [26] and enzyme-linked immunosorbent assays (ELISA) [27]. These assays are however often limited by time-consuming and complicated radio and fluorescent labeling protocols, excessive use of sample and auxiliary reagents, and poor long-term stability and shelf-life [28]. Moreover, prolonged incubation times typically result in slow diagnostic turnaround (3–11 days), which renders these methods rather ineffective for therapeutic management of AVP.

These issues can be mitigated with highly sensitive and label-free microfluidic biosensors that specifically isolate and detect AVP; however, to our knowledge, such devices have yet to be demonstrated. This opportunity is explored in the present paper, in which we demonstrate the specific aptameric isolation and enrichment, as well as label-free MALDI–MS detection, of AVP. Using a microfluidic device we recently developed [29], AVP is first selectively captured and enriched on an aptamer-functionalized solid phase, and then collected by thermally induced isocratic elution (i.e., elution within the same aqueous phase for analyte capture) on a MALDI sample plate for mass spectrometric analysis. We first use fluorescently labeled AVP to systematically characterize the time response, concentration dependence and thermally induced dissociation of aptamer–AVP binding, as well as the continuous-flow enrichment of dilute AVP samples. We then perform label-free detection of AVP, in the presence of significant levels of model impurities, at both physiologically critical concentrations (i.e., during symptoms of immunological shock and renal congestive heart failure) and normal conditions. Our approach is shown to drastically reduce the required time to detect AVP to within several hours (compared to 3–11 days for conventional approaches [26,27]), while eliminating the needs for fluorescent or radiometric labeling. As such, this work provides a foundation for point-of-care and automated diagnosis of AVP syndromes.

2. Design and fabrication

The microfluidic aptasensor consists of a microchamber packed with aptamer-functionalized microbeads for sample purification, a microheater and temperature sensor for thermally induced analyte release, and microchannels equipped with a surface tension-based passive microflow gate and air vent for transferring released sample to a spotting outlet coupled to a MALDI sample plate (Fig. 1a) [29]. The device is realized by a glass slide bonded to three stacked polymer layers (Fig. 1b): the bottom-layer incorporates the inlets, passive flow gate, and waste outlet; the middle layer contains the air vent and seals the bottom-layer microfluidic features; and the top layer defines the spotting outlet, to which a glass capillary is fitted to allow sample ejection to a MALDI sample plate. The top layer also houses the air vent channel, whose hydrophobic surface allows trapped gas bubbles and dead volumes to be eliminated from the spotting outlet. Microbeads on which aptamer molecules are immobilized are packed inside the microchamber (volume: 1.6 μl) and retained by narrow slits. A thin-film resistive metal heater and temperature sensor are integrated on the glass surface to allow on-chip, closed-loop temperature control.

During operation, an aqueous sample containing AVP potentially intermixed with non-target molecules is introduced into the aptamer microchamber, and thus is extracted by the aptamer. This occurs at a suitable temperature (~37 °C) so that the aptamer specifically captures the target from the liquid-phase while impurities are flushed from the system through the waste outlet. The above sequence is repeated in a continuous fashion in order to adequately purify and enrich the analyte, if necessary. For MALDI–MS

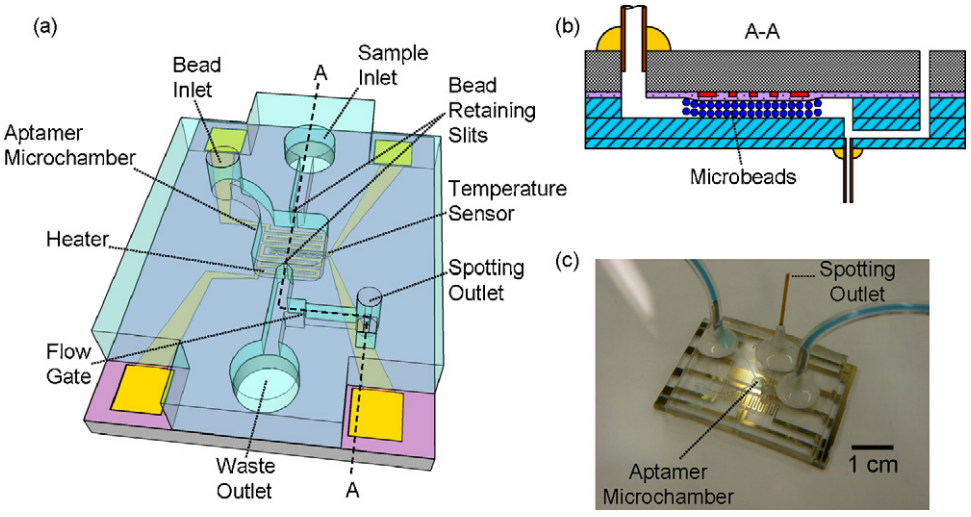

Fig. 1. (a) A schematic of the microfluidic aptasensor. (b) Cross-sectional view along line A–A from (a) illustrating the device's layered structure. (c) A photograph of a packaged device.

analysis, the aptamer interaction mechanisms can be disrupted by altering the temperature of the solid support, such that the concentrated analyte is released into a plug of pure MALDI matrix solution. Subsequently, the microflow gate is utilized to transfer the plug to the spotting outlet by exploiting the pressure difference induced across an air–liquid interface in a hydrophobic channel restriction. If the pressure drop between the sample inlet and the flow gate exceeds this pressure difference, fluid will enter the secondary channel leading to the spotting outlet. Hence, the fluid can be switched between the channels that access the spotting outlet or bypass it to the waste outlet [30]. Thus, purified and enriched samples are ejected from the capillary tip by hydrodynamic force and allowed to crystallize before mass spectrometry analysis. This preceding protocol allows isocratic elution of analytes onto a MALDI sample plate for MS detection. Returning the temperature to the initial state allows the aptamer to revert to its initial functional structure, i.e., the aptamer-functionalized surfaces are regenerated.

The device was fabricated by standard soft lithography techniques [31]. Briefly, sheets of polydimethylsiloxane (PDMS) bearing the microfluidic features were obtained by micromolding using a master fabricated from SU-8 on silicon, while the microheater and temperature sensor were fabricated from a 100 nm gold thin film (using a 5 nm chromium adhesion layer) on glass. Each PDMS sheet was then bonded to the glass chip, as shown in Fig. 1b, after treating the bonding interfaces by oxygen plasma.

3. Experimental methods

Our experiments involved systematic device characterization using fluorescently labeled AVP with respect to adenosine monophosphate (AMP) as a model impurity, and demonstration of capture, enrichment and MALDI–MS detection of unlabeled AVP from AMP. The AVP-specific aptamer, termed a spiegelmer, was derived from a prior literature report (5′-GGGGUAGGGCUUGGAUGGGUAGUACACGUGUGCGUGGU-3′) [32] and resists degradation by a selection process involving enantiomeric RNA mirror imaging. It was custom synthesized and biotinylated by ChemGenes Corporation. Meanwhile, unlabeled AVP and AVP labeled with the fluorescent dye Tamra (TMR-AVP) were synthesized through American Peptide Company. Unlabeled AMP was obtained from Sigma while AMP labeled with the fluorescent dye thiazole orange (TO-AMP) was prepared in-house. Analytical samples used during fluorescently based characterization experiments involving TMR-AVP were prepared in buffer solution (AVP-buffer, pH 7.4) consisting of purified water (sterile RNase/Protease-free from Fisher), Tris–HCl (20 mM), NaCl (150 mM), KCl (5 mM), $CaCl_2$ (1 mM), and $MgCl_2$ (1 mM); while samples utilized in MALDI–MS protocols required solvation in only purified water (compounds acquired through Fisher). A MALDI matrix, cyano-4-hydroxycinnamic acid (Sigma) was solvated in a volume ratio mixture of 50:50:0.3 purified water/acetonitrile/trifluoroacetic acid. Porous bis-acrylamide beads, copolymerized with azlactone (50–80 μm in diameter) and coated with UltraLink streptavidin, were acquired from Pierce and used to immobilize spiegelmer via a biotin-streptavidin link. These beads were packed in the microchamber and held by narrow slits 40 μm in width. We used the relatively large bead sizes to facilitate the proof-of-concept, which can be considerably decreased by reducing the bead-retaining slit width as well as the microchamber volume.

Devices were initially rinsed thoroughly (flow rate: 10 μl/min) with purified water for 30 min (similar for subsequent rinses in all experiments). Sample solutions in varying concentrations of TMR-AVP and unlabeled AVP were prepared using the appropriate mass weights of the respective compound and either AVP-buffer (for TMR-AVP), or water (for AVP) solution. Manual pressure was utilized to pack microbeads from the bead introduction channel of the aptasensor into the microchamber. After another rinse step, an AVP–aptamer solution (50 μM) was injected (3 μl, 50 μl/min) and allowed to incubate (40 min) in the chamber. (This procedure was used for all sample injections.) A Nikon Eclipse TE300 was utilized for fluorescence characterization. Initially, a baseline fluorescence signal was acquired by focusing a 10× objective at a central location in the extraction chamber and averaging an 8-bit RGB signal over the entire recorded fluorescence image. Alternatively, MALDI–MS experiments were performed using a time of flight mass spectrometer (Applied Biosystems, Voyager, DE).

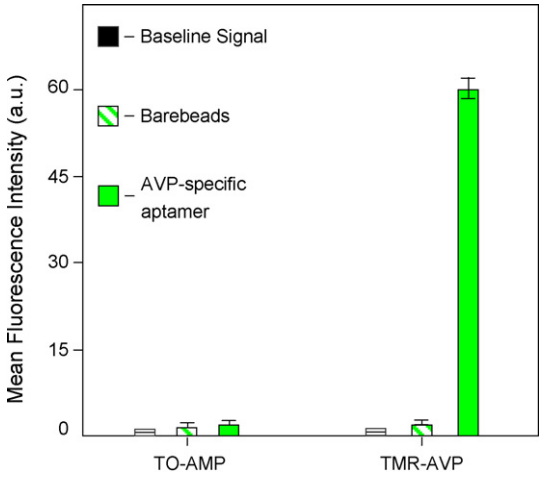

Fig. 2. Control experiments. A 1 μM sample of TMR-AVP and TO-AMP are introduced into the aptasensor microchamber containing bare beads.

4. Results and discussion

We first performed systematic characterization of the AVP–aptamer binding using TMR-AVP (peak absorption: 540 nm; peak emission: 580 nm), and then carried out experiments by MALDI–MS analysis. The fluorescently based characterization allowed us to visualize the binding characteristics of the system and gain insight into later experiments involving MALDI–MS analysis.

4.1. Experimental controls

Several control experiments were performed, in which the microchamber with and without AVP–aptamer-functionalized beads, were introduced to samples of TMR-AVP and a model impurity, TO-AMP (peak absorption: 480 nm; peak emission: 530 nm). After a baseline fluorescence signal was acquired, the microchamber was initially packed with non-functionalized beads (only streptavidin-coated microbeads: “bare beads”). Subsequently, samples of TMR-AVP and TO-AMP (1 μM) were injected into the microchamber and the resulting fluorescence gain was measured. Similarly, TMR-AVP and TO-AMP samples (1 μM) were exposed to a microchamber packed with AVP–aptamer-functionalized microbeads. As shown in Fig. 2, there was no appreciable signal above the baseline in the bare beads case for both TMR-AVP and TO-AMP samples, while only a slight increase (1.45%) in fluorescence over the baseline when TO-AMP was introduced to AVP–aptamer. This could be attributed to non-specific adsorption to the microbeads by TO-AMP. In contrast, the fluorescent intensity from introducing TMR-AVP to AVP–aptamer was dominant, as expected. It can thus be concluded that TMR-AVP indeed interacts with AVP–aptamer and moreover, this result highlighted the specificity between the binding of AVP–aptamer and AVP.

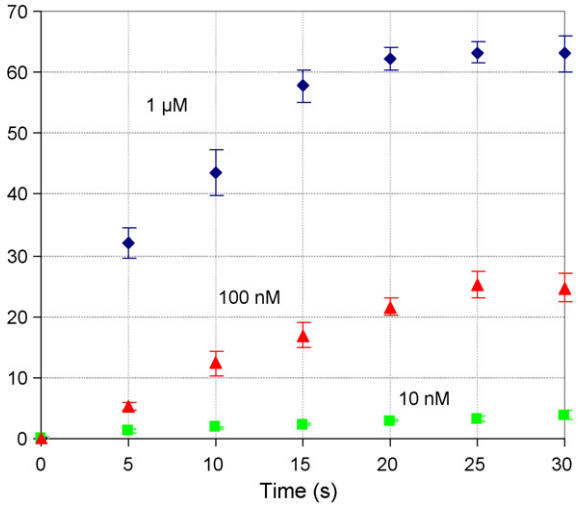

Fig. 3. Time-resolved fluorescence measurements for the binding of TMR-AVP to the aptamer. Longer incubation times were required for lower concentration samples, as predicted by monovalent equilibrium binding theory [27].

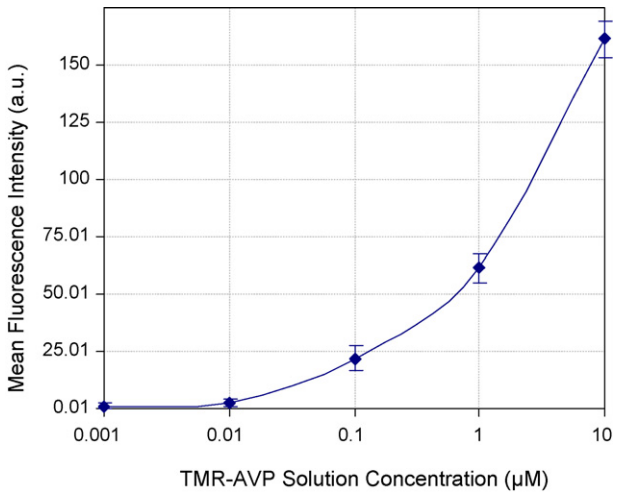

Fig. 4. Concentration dependent fluorescence response of TMR-AVP at varying concentrations. A sample was injected into and incubated in the extraction chamber. At this point, TMR emission was measured from the objective lens and recorded. A dose dependent relationship was observed.

4.2. Time-resolved measurement of aptamer and AVP binding

The time course of affinity capture of TMR-AVP by the aptamer was obtained to observe the kinetic behavior of the system. This was accomplished by recording the time-resolved fluorescence response after introducing a TMR-AVP sample into the aptamer microchamber. Fluorescence micrographs were taken at discrete time intervals (5 s) following an injection of TMR-AVP in varying concentrations (0.01, 0.1, and 1 μM). To reduce the effect of fluorescent photobleaching, the shutter to the mercury lamp was closed for the time period between all signal measurements. Fluorescence signal measurements were obtained, averaged and then plotted as a function of time (Fig. 3). In all experiments, the fluorescence intensity increased steadily with time until sufficient signal saturation occurred. The apparent AVP capture time (i.e., time constant for the observed time course of AVP capture) was approximately 8.4, 13.5, and 22.1 s for 1, 0.1, and 0.01 μM TMR-samples, respectively. Generally, the binding time may be affected by three time scales: thermal, diffusion and kinetic. For the porous microbead-packed microchamber, the diffusion time scale was estimated to be $d^2/D \sim 5.85$ s, where d is the average bead diameter (50 μm), and D the analyte diffusivity (estimated for AVP to be $\sim 4 \times 10^{-6}$ cm^2/s). This is significant compared with the apparent analyte capture times seen in Fig. 3. Thus, the interaction between AVP and its aptamer in this situation may depend on both kinetics and diffusion, which will be further investigated in future work by possibly modeling the aptamer–AVP binding interaction. Further, the longer apparent capture times observed for lower AVP concentrations agrees with that predicted by monovalent binding theory (which is believed to be the case for AVP) [33]. In experiments reported below, these apparent capture times provided a basis for our choice of the sample incubation time (for concentration dependent fluorescence response) or infusion flow rate (for analyte enrichment).

4.3. Concentration dependent capture of TMR-AVP

To confirm aptamer-based capture of AVP within the aptasensor microchamber, solutions of TMR-AVP at five different concentrations (0.001, 0.01, 0.1, 1, and 10 μM) were injected into the microchamber. After each sample introduction, fluorescence yield was quantified after an initial 30 s incubation time to assure equilibrium sample binding. Following the extraction of AVP, the microchamber was washed with buffer to rid all non-specific compounds, un-reacted molecules, and impurities. Results are presented in Fig. 4. It can be seen that below 1 nM, no measurable signal above the baseline was detected. Concentrations at and above 1 nM, however, were readily detectable for the aptasensor with ca. a signal-to-noise ratio of 3. Additionally, the concentration dependent fluorescence signal produced through TMR-AVP capture appeared to be dose-responsive [34], as signified by the S-shape fit of the data using GraphPad Prism 5 (GraphPad Software) software. These results suggested the need for enhanced detection techniques, such as analyte enrichment, in order to render the aptasensor clinically viable; in other words, enable detection of AVP below 1 nM at physiologically and clinically relevant levels (e.g., 1–500 pM).

4.4. Enhanced detection of TMR-AVP by analyte enrichment from a dilute sample

To investigate detection enhancement of TMR-AVP, a continuous-flow analyte enrichment scheme was adopted. Specifically, a dilute solution of TMR-AVP (100 pM) was continuously infused into the microchamber until fluorescence saturation was observed. Taking into consideration the required residence time determined in Section 4.2, the sample flow rate was chosen to be 15 μl/min (corresponding to a sample residence time of 20 s in the microchamber) to insure complete AVP interaction with the aptamer. Fluorescence signals were obtained periodically (every 60 min) until approximately 480 min, when no significant increase in fluorescence was observed, which suggested saturation (Fig. 5). This agrees with the expected equilibrium condition that concentration of a molecular analyte onto a receptor modified surface increases consistently with time at a decreasing rate. Moreover, the observed fluorescence response of the original 100 pM sample corresponds to the apparent fluorescence response of a 0.1 μM TMR-AVP sample, indicating significant detection enhancement. Hence, using the analyte enrichment feature of the aptasensor demonstrated clinical potential for vasopressin diagnostics since shock and congestive heart failure AVP signaling levels in plasma are ca. 100–500 pM. Moreover, it is significant to note that the required processing time to perform enhanced detection of TMR-AVP with the aptasensor, although seemingly long (8 h), is drastically improved over conventional techniques, which require nearly 11 days.

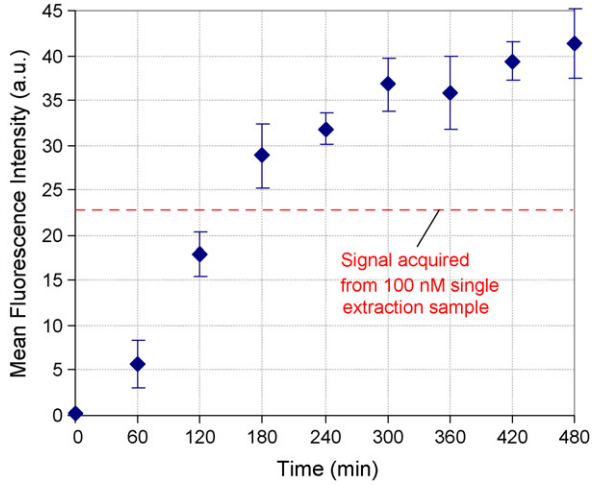

Fig. 5. Enrichment by continuous infusion of a dilute sample (100 pM) of TMR-AVP. The red dashed line indicates the relative fluorescence of a 100 nM sample acquired in Section 4.3. This experiment highlighted the capability of enrichment prior to detection for enhanced signal acquisition. Insight was also gained for the time required for saturation.

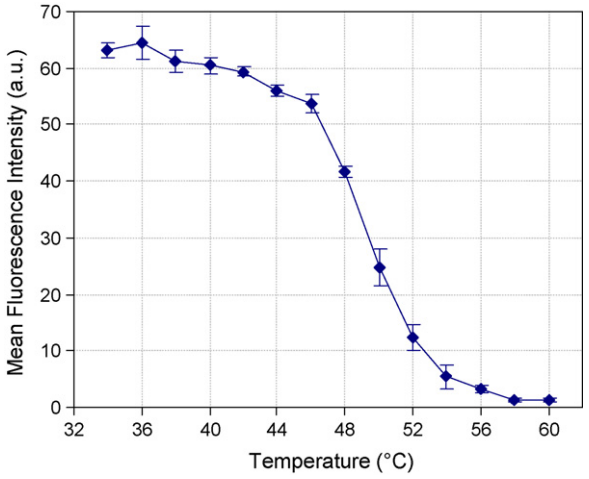

Fig. 6. Thermally activated release of captured TMR-AVP. An initial 1 μM sample of TMR-AVP was captured from solution at ~35 °C. Subsequently, the temperature was raised incrementally while introducing pure AVP-buffer. Notice the initiation of a sharp decrease in signal at ~46 °C, which continues to vanish as the temperature increases implying release of the TMR-AVP from the aptamer.

4.5. Thermally activated dissociation of TMR-AVP binding

Characterization of the temperature-dependant reversibility of AVP and AVP–aptamer binding was studied in order to enable investigation of label-free MALDI–MS detection. This was accomplished in our device by thermally activated release and isocratic elution of analytes from aptamer-functionalized microbeads. To demonstrate this, a 1 μM TMR-AVP solution was first introduced into the microchamber and allowed to associate with AVP–aptamer. After binding of TMR-AVP on the aptamer surface, a high intensity fluorescence signal was observed (Fig. 6). The temperature on-chip was then increased to a predetermined setpoint and held for 2 min while AVP-buffer was flowed into the microchamber. We repeated the experiment for several elevated setpoint temperatures ranging from 34 to 60 °C. A sharp decrease (93%) in fluorescence intensity occurred at 50 °C that continued until fully suppressed at 58 °C, indicating nearly complete reversal of TMR-AVP binding on the microbeads. (The effect of photobleaching was determined to be negligible within the time scales of this experiment.) In general, as aptamers bind to their ligand counterparts, the resulting complex demonstrates better thermal stability than that of the uncomplexed state [35]. It is inferred that binding between spiegelmer and AVP involves specific insertion of the polypeptide within a G-quartet structure formed in the

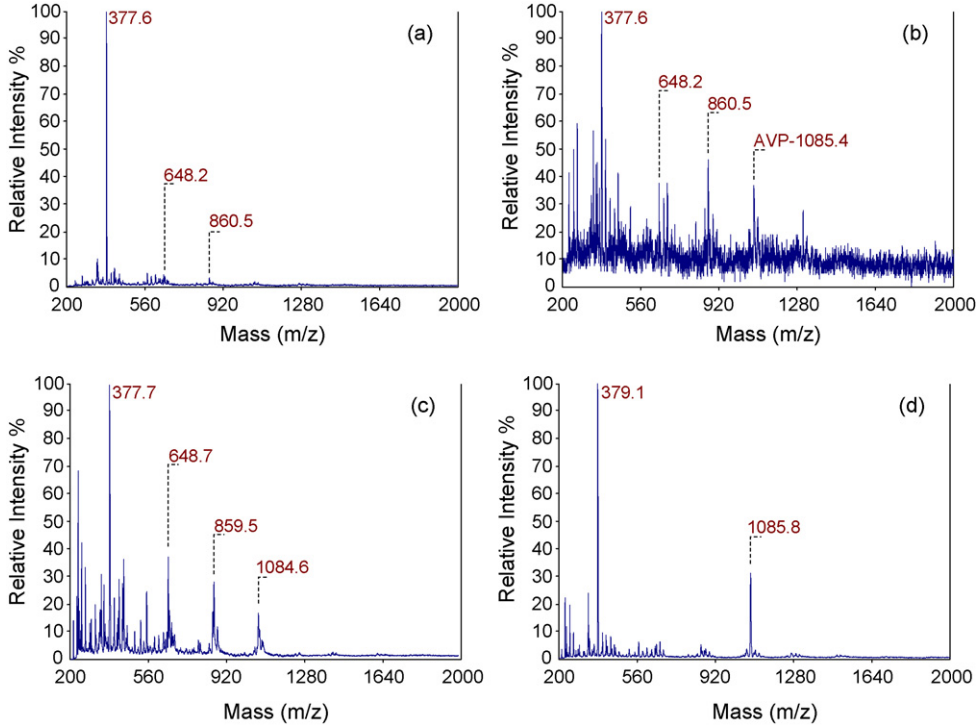

Fig. 7. Detection of unlabeled AVP using aptasensor. A sample of AVP is introduced into the aptasensor for capture inside the microchamber, followed by thermally induced isocratic elution into a pure matrix plug that is subsequently spotted onto the MALDI plate. Mass spectra of (a) 1 pM AVP; (b) 10 pM; (c) 100 pM; 1 nM (d).

spiegelmer sequence, resulting in thermally stable interaction [32]. As aptamers are known to exhibit highly stimuli-dependent secondary and tertiary binding structures [36], we speculate that, to a significant degree, the thermal energy (above 50 °C) imparted to the spiegelmer disrupts this G-quartet to prevent binding with AVP. Furthermore, it is possible that the additional thermal energy promotes dehydration, which disrupts van der Waals interactions and hydrogen bonding at the spiegelmer–AVP binding interface. These results established the capability of our aptasensor for thermally activated release and isocratic elution of a captured target. Moreover, we exploited this technique to perform repeated experiments with TMR-AVP samples within the same aptasensor chip. The fluorescence signals resulting from TMR-AVP extraction and release in all experimental testing produced consistent and repeatable values, as reflected by the error bars on all the data. This indicates that the thermal stimulation did not affect the functionality of the aptamer molecules and successfully allowed aptasensor regeneration and repeated use.

4.6. Extraction, thermally induced release and MALDI–MS detection of AVP

To demonstrate the ability to extract and detect AVP by MALDI–MS using our aptasensor, we first introduce discrete samples of physiologically relevant concentrations of AVP (1 pM, 10 pM, 100 pM, and 1 nM) into the chamber. After interaction with the aptamer-functionalized beads, the AVP molecules are thermally released and transferred to the spotting outlet via the passive microflow gate and finally deposited onto a MALDI–MS plate. Mass analysis follows (Fig. 7). No molecular ion peak was registered for the 1 pM sample (Fig. 7a). In fact, only mass peaks corresponding to the HCCA matrix and its fragments/adducts were present (377.6, 648.2 and 860.5 Da/z). However, the mass spectra of a spots obtained for all other AVP solutions (Fig. 7b–d) shows a distinctive molecular ion peak of 1084.4 Da/z that corresponds to AVP. For example, sample AVP concentrations between 10 pM and 1 nM (Fig. 7b–d) demonstrated improved detection and signal-to-noise ratio with increasing concentration. However, since AVP concentration was still relatively low for sample concentrations between 10 pM and 1 nM, the magnitude of its peak was still smaller than the MALDI matrix peaks (e.g., 377.6 Da/z). We additionally tested the aptasensor with concentrations higher than 1 nM (up to 100 μM, data not shown), and observed significant improvement in the signal-to-noise ratio as well as the analyte-to-matrix peak contrast. In these cases, the AVP peak dominates matrix peak amplitudes. Data shown here indicates that the potential native detection limit of the aptasensor lies between 1 and 10 pM. Moreover, this detection sensitivity is ca. on the order of average physiological AVP levels in plasma [24]. To improve detection at low levels (e.g., 1–100 pM) analytes can also be enriched in the aptasensor prior to MALDI–MS.

4.7. Enhancement of AVP detection by enrichment of a dilute sample

Naturally occurring hormonal vasopressin is present in plasma predominantly above 1 pM [25]. To demonstrate detection at this level and therefore pervade all clinical settings, we investigated the ability of our aptasensor to enrich poorly, or undetectable, samples of AVP using continuous infusion of an original dilute AVP solution. Insight gained from Section 4.4 was employed to establish particular protocol parameters, such as saturation time (~8 h) and flow rate (15 μl/min). Following a similar process, dilute samples of AVP (1, 10, and 100 pM) were continuously infused into the aptamer chamber for the designed time period. This was followed by thermally induced release of the captured AVP into a pure matrix solution (1 μl), and subsequent transfer of the enriched analyte plug to the spotting outlet. A mass spectrum was obtained from the resulting sample spot (Fig. 8). For each original dilute sample, there appeared to be an enhanced detection of the molecular ion peak for AVP. Specifically, the original 1, 10 and 100 pM samples produced mass spectra where the AVP peak compared to (or was better than, in the case of the 100 pM sample) 100 pM, 1 nM, and 100 nM samples measured in Section 4.6, respectively. Notably, the 1 pM sample, which was undetectable before analyte enrich-

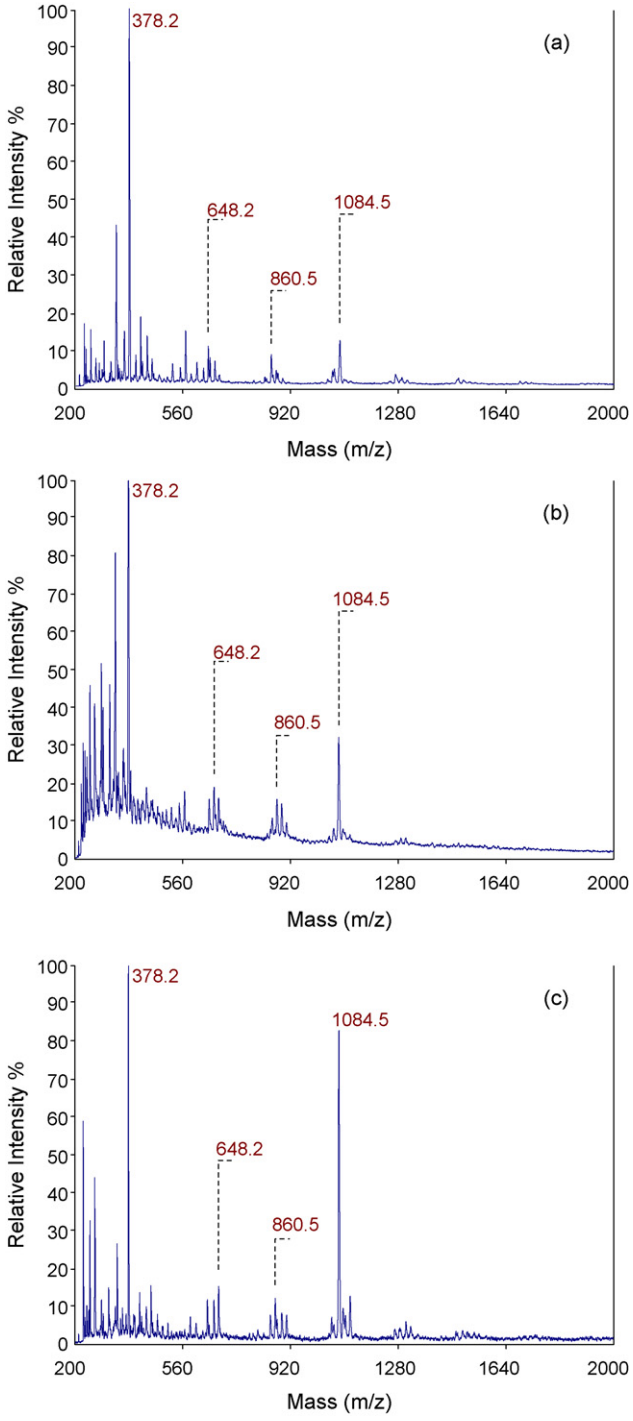

Fig. 8. Enrichment of dilute AVP samples by continuous infusion of prior to MALDI–MS detection: (a) 1 pM; (b) 10 pM; 100 pM (c). Here, the ability to increase the relative signal intensity of the molecular ion peak for AVP for ultralow concentration samples demonstrates the utility of the microfluidic enrichment process.

ment, became quantifiable afterwards. These results establish the capabilities of our aptasensor for enhancing the detection of low concentration analytes so as to facilitate label-free detection by MALDI–MS. More importantly, this also highlights the capabilities of the aptasensor within the full range of physiologically relevant concentrations of AVP. Furthermore, although the repeated use of the aptasensor is not explicitly gleaned from the presented data (due to the limits of presenting spectroscopic data), the aptasensor was easily regenerated (using thermal stimulation of the aptamer-functionalized beads) to allow reuse and repeated functionality (see Section 4.5).

5. Conclusion

Microfluidic aptasensors hold significant potential in addressing the needs of real world clinical diagnostics and therapeutics for low abundance detection and analysis of biomolecules. Here, we demonstrated a microfluidic approach that utilizes a thermally responsive affinity aptamer, specific to arginine vasopressin, for highly selective enrichment, isocratic elution, and label-free detection with integrated MALDI–MS. Arginine vasopressin is typically responsible for osmotic regulation of water in vivo, but can serve as a biomarker for diagnosing immunological shock, as a result of sepsis, or congestive heart failure. Initially, systematic characterization of the aptasensor was performed using fluorescently labeled AVP, which provided insight and information for subsequent label-free experiments. We then investigated MALDI–MS detection of AVP approaching 10 pM without prior enrichment, and 1 pM following continuous enrichment of a dilute sample. The aptasensor offers distinct advantages over existing techniques used to detect AVP levels, such as ultrasensitive detection, uncomplicated protocols free of chemical labeling steps or auxiliary reagents, and prolonged sensor stability. Such qualities are lacking in ELISA and IRA bioassays currently employed to diagnose AVP-specific conditions. Moreover, detection times in our approach are drastically reduced from up to 11 days to several hours. This demonstrates the clinical potential of the microfluidic aptasensor, for example in ICU settings where the diagnosis of sepsis shock must be performed in a timely manner.

As a proof-of-concept, our investigation was focused on AVP detection within conditioned samples only (i.e., pure buffers or purified water, free from proteases or peptide digesting enzymes). Future work will address obstacles encountered with clinical samples. One such example is the detection of AVP in biological samples, such as human serum. Such samples are difficult to handle due to impediments such as vasopressin being susceptible to biofouling and degradation by enzymes present in plasma. This issue could be resolved by, for example, using a pre-filtration stage to remove large plasma proteins and enzymes from the sample prior to its introduction into the microfluidic aptasensor, or spiking the sample with protease inhibitors or blockers to minimize the digestive degradation of AVP. Additionally, it is important in future work to improve the reliability and consistency of AVP quantification with MALDI–MS. This can be achieved by fine tuning of sample spot homogeneity and applied laser power of the mass spectrometer. Sample spot homogeneity depends on preferential solubility factors for the analyte in question. For AVP, a relatively hydrophilic polypeptide, a polar solvent would suffice. With these improvements, the microfluidic aptasensor will allow sensitive and specific detection of AVP in clinical samples, providing a truly practical diagnostic tool for vasopressin-related medical conditions.

Acknowledgments

We gratefully acknowledge financial support from the National Science Foundation (CBET-0693274, CBET-0854030 and EIA-0324845) and the Alternatives Research and Development Foundation.

References

[1] J.H.T. Luong, K.B. Male, J.D. Glennon, Biosensor technology: technology push versus market pull, Biotechnology Advances 26 (2008) 492–500.
[2] D.H.J. Bunka, P.G. Stockley, Aptamers come of age—at last, Nature Reviews Microbiology 4 (2006) 588–596.
[3] C. Tuerk, L. Gold, Systematic evolution of ligands by exponential enrichment: RNA ligands to bacteriophage T4 DNA polymerase, Science 249 (1990) 505–510.
[4] C. Manironi, A. DiNardo, P. Fruscoloni, G.P. Tocchini-Valentini, In vitro selection of dopamine RNA ligands, Biochemistry 36 (1997) 9726–9734.
[5] D. Nieuwlandt, M. Wecker, L. Gold, In-vitro selection of RNA ligands to substance-P, Biochemistry 34 (1995) 5651–5659.
[6] S.E. Lupold, B.J. Hicke, Y. Lin, D.S. Coffey, Identification and characterization of nuclease-stabilized RNA molecules that bind human prostate cancer cells via the prostate-specific membrane antigen, Cancer Research 62 (2002) 4029–4033.
[7] P. Burgstaller, A. Girod, M. Blind, Aptamers as tools for target prioritization and lead identification, Drug Discovery Today 7 (2002) 1221–1228.
[8] L.S. Green, C. Bell, N. Janjic, Aptamers as reagents for high-throughput screening, Biotechniques 30 (2001) 1094.
[9] E.N. Brody, M.C. Willis, J.D. Smith, S. Jayasena, D. Zichi, L. Gold, The use of aptamers in large arrays for molecular diagnostics, Molecular Diagnosis 4 (1999) 381–388.
[10] S.M. Nimjee, C.P. Rusconi, R.A. Harrington, B.A. Sullenger, The potential of aptamers as anticoagulants, Trends in Cardiovascular Medicine 15 (2005) 41–45.
[11] P.J. Conroy, S. Hearty, P. Leonard, R.J. O'Kennedy, Antibody production, design and use for biosensor-based applications, Seminars in Cell & Developmental Biology 20 (2009) 10–26.
[12] S. Jayasena, Aptamers: an emerging class of molecules that rival antibodies in diagnostics, Clinical Chemistry 45 (1999) 1628–1650.
[13] L.J. Lee, S.T. Yang, S.Y. Lai, Y.L. Bai, W.C. Huang, Y.J. Juang, Microfluidic enzyme-linked immunosorbent assay technology, Advances in Clinical Chemistry 42 (2006) 255–295.
[14] A. Bange, H.B. Halsall, W.R. Heineman, Microfluidic immunosensor systems, Biosensors & Bioelectronics 20 (2005) 2488–2503.
[15] S. Cho, S.H. Lee, W.J. Chung, Y.K. Kim, Y.S. Lee, B.G. Kim, Microbead-based affinity chromatography chip using RNA aptamer modified with photocleavable linker, Electrophoresis 25 (2004) 3730–3739.
[16] W.J. Chung, M.S. Kim, S. Cho, S.S. Park, J.H. Kim, Y.K. Kim, B.G. Kim, Y.S. Lee, Microaffinity purification of proteins based on photolytic elution: toward an efficient microbead affinity chromatography on a chip, Electrophoresis 26 (2005) 694–702.
[17] J.S. Swensen, Y. Xiao, B.S. Ferguson, A.A. Lubin, R.Y. Lai, A.J. Heeger, K.W. Plaxco, H.T. Soh, Continuous, real-time monitoring of cocaine in undiluted blood serum via a microfluidic, electrochemical aptamer-based sensor, Journal of the American Chemical Society 131 (2009) 4262–4266.
[18] J.P. Hilton, T.H. Nguyen, R. Pei, M. Stojanovic, Q. Lin, A microfluidic affinity sensor for detection of cocaine, Sensors and Actuators A: Physical, submitted for publication.
[19] C.A. Savran, S.M. Knudsen, A.D. Ellington, S.R. Manalis, Micromechanical detection of proteins using aptamer-based receptor molecules, Analytical Chemistry 76 (2004) 3194–3198.
[20] M.D. Schlensog, T.M.A. Gronewold, M. Tewes, M. Famulok, E. Quandt, A Love-wave biosensor using nucleic acids as ligands, Sensors and Actuators B: Chemical 101 (2004) 308–315.
[21] H.M. So, K. Won, Y.H. Kim, B.K. Kim, B.H. Ryu, P.S. Na, H. Kim, J.O. Lee, Single-walled carbon nanotube biosensors using aptamers as molecular recognition elements, Journal of the American Chemical Society 127 (2005) 11906–11907.
[22] S.X. Huang, Y. Chen, Ultrasensitive fluorescence detection of single protein molecules manipulated electrically on Au nanowire, Nano Letters 8 (2008) 2829–2833.
[23] C.L. Holmes, B.M. Patel, J.A. Russell, K.R. Walley, Physiology of vasopressin relevant to management of septic shock, Chest 120 (2001) 989–1002.
[24] E.A. Zimmerman, The organization of oxytocin and vasopressin pathways, Advances in Biochemical Psychopharmacology 28 (1981) 63–75.
[25] D. Morales, J. Madigan, S. Cullinane, J. Chen, M. Heath, M. Oz, J.A. Oliver, D.W. Landry, Reversal by vasopressin of intractable hypotension in the late phase of hemorrhagic shock, Circulation 100 (1999) 226–229.
[26] C.G. Beardwell, Radioimmunoassay of arginine vasopressin in human plasma, Journal of Clinical Endocrinology and Metabolism 33 (1971) 254–260.
[27] J. Proux, A. Baskali, C. Remy, C. Creminon, P. Pradelles, Development of an enzyme-immunoassay for arginine-vasopressin (AVP)-like insect diuretic hormone, Comparative Biochemistry and Physiology B-Biochemistry & Molecular Biology 106 (1993) 659–666.
[28] C.K. O'Sullivan, Aptasensors—the future of biosensing, Analytical and Bioanalytical Chemistry 372 (2002) 44–48.
[29] T. Nguyen, R. Pei, M. Stojanovic, D. Landry, Q. Lin, A microfluidic aptasensor with integrated sample preconcentration, isocratic elution and mass spectrometric detection, in: International Conference on Solid-State Sensors, Actuators and Microsystems (Transducers '09), Denver, CO, United States, 2009, pp. 1822–1825.

[30] Y.Y. Feng, Z.Y. Zhou, X.Y. Ye, H.J. Xiong, Passive valves based on hydrophobic microfluidics, Sensors and Actuators A-Physical 108 (2003) 138–143.
[31] M.A. Unger, H.-P. Chou, T. Thorsen, A. Scherer, S.R. Quake, Monolithic microfabricated valves and pumps by multilayered soft lithography, Science 288 (2000) 113–116.
[32] W.G. Purschke, D. Eulberg, K. Buchner, S. Vonhoff, S. Klussmann, An L-RNA-based aquaretic agent that inhibits vasopressin in vivo, Proceedings of the National Academy of Sciences of the United States of America 103 (2006) 5173–5178.
[33] D.A. Lauffenburger, J.J. Linderman, Receptors: Models for Binding, Trafficking, and Signaling, Reprint, Illustrated ed., Oxford University Press, New York, 1996.
[34] E.J. Calabrese, Biological effects of low level exposures dose–response relationships, in: Research on the Biological Effects of Low Level Exposure (BELLE) to Chemical Agents and Radioactivity, Crystal City, VA, USA, 1994, p. 320.
[35] P.H. Lin, S.L. Yen, M.S. Lin, Y. Chang, S.R. Louis, A. Higuchi, W.Y. Chen, Microcalorimetrics studies of the thermodynamics and binding mechanism between L-tyrosinamide and aptamer, Journal of Physical Chemistry B 112 (2008) 6665–6673.
[36] T. Mairal, V.C. Ozalp, P.L. Sanchez, M. Mir, I. Katakis, C.K. O'Sullivan, Aptamers: molecular tools for analytical applications, Analytical and Bioanalytical Chemistry 390 (2008) 989–1007.

Biographies

ThaiHuu Nguyen received his B.Sci. from the University of Virginia in 2005, majoring in Aerospace Engineering. He received his M.S. from Columbia University in Mechanical Engineering in 2007. He is currently a Ph.D. candidate in Mechanical Engineering at Columbia University, and his research interests include integrating aptamers in microfluidic platforms for biochemical and biomedical related applications.

Renjun Pei received his B.Sci. degree in 1993 and Ph.D. degree in 1998 in the Department of Chemistry from Wuhan University, PR China. Dr. Pei held a JSPS postdoctoral fellowship in 2001–2003 in the Institute for Chemical Research, Kyoto University, Japan. He is currently working in the Department of Medicine, Columbia University. His research interests include aptamers, light-up probes, allosteric deoxyribozymes, molecular robotics, and bio-/nanotechnologies.

Donald W. Landry received his B.Sci. in chemistry from Lafayette College (1975), followed by his Ph.D. in organic chemistry from Harvard University (1979). He then completed an M.D. at Columbia University, College of Physicians and Surgeons in 1983 and was a resident from 1983 to 1985 at Harvard Medical School, Massachusetts General Hospital. Professor Landry is currently the chair of the Department of Medicine Columbia University, College of Physicians and Surgeons, as well as the Director of the Divisions of Nephrology and Clinical Pharmacology and Experimental Therapeutics.

Milan N. Stojanovic obtained his B.Sci. at Beogradski Univerzitet, Serbia and Ph.D. in organic chemistry at Harvard University, USA. After a postdoctoral fellowship at Columbia University, Department of Medicine, he remained there as a faculty member.

Qiao Lin received his Ph.D. in mechanical engineering from the California Institute of Technology in 1998 with thesis research in robotics. Dr. Lin conducted postdoctoral research in microelectromechanical systems (MEMS) at the Caltech Micromachining Laboratory from 1998 to 2000, and was an Assistant Professor of Mechanical Engineering at Carnegie Mellon University from 2000 to 2005. He has been an Associate Professor of Mechanical Engineering at Columbia University since 2005. His research interests are in designing and creating integrated micro-/nanosystems, in particular MEMS and microfluidic systems, for biomedical applications.